

Anomalous Quartic Gauge Couplings from Six Quark Production

Erik Schmidt, Michael Beyer, and Henning Schröder
*Institute of Physics, University of Rostock,
 18051 Rostock, Germany*

(Dated: October 29, 2018)

The absence of a light Higgs boson causes vector boson couplings to become strong at 1 TeV. A general framework for a systematic and consistent treatment is provided by effective theories of electroweak symmetry breaking. Already in next-to-leading order there appear quartic gauge couplings that go beyond the standard model and are hence called anomalous. We investigate intermediate three gauge boson states W^+W^-Z and ZZZ occurring in six quark production in electron positron collisions under the conditions of the International Linear Collider. We perform a sensitivity analysis of the relevant anomalous quartic gauge couplings presenting their expected limits.

PACS numbers: 11.15.Ex, 11.30.Qc, 12.15.-y, 12.39.Fe

I. INTRODUCTION

One important objective of future accelerator experiments is to unveil the mechanism behind electroweak symmetry breaking (EWSB). In this respect generic effective field theories are a proper choice for a systematic and consistent treatment. These theories arise in a natural way, if no light Higgs is assumed to be present in the particle spectrum [1]. Including all operators obeying the underlying symmetries, these effective theories are non-renormalizable in a narrow sense. At each order of perturbation theory more counterterms have to be introduced in order to render the whole theory finite. These so called anomalous couplings parameterize the effects of new physics in a generic, model independent way. Since the construction of the theory starts from the known low energy behavior of the electroweak interaction, the way of describing EWSB is called the bottom-up approach, see e.g. ref. [2]. Alternatively, the top-down approach constitutes the whole particle spectrum and symmetries of the theory at high energies from the beginning by constructing renormalizable Lagrangians.

In the following we consider the interaction between four bosons, in particular production of intermediate three boson states. The relevant CP conserving operators arising in next-to-leading-order are the two $SU(2)_V$ -conserving [3]

$$\mathcal{L}_4 = \frac{\alpha_4}{16\pi^2} \text{Tr}(V_\mu V_\nu) \text{Tr}(V^\mu V^\nu) \quad (1)$$

$$\mathcal{L}_5 = \frac{\alpha_5}{16\pi^2} \text{Tr}(V^\mu V_\mu)^2, \quad (2)$$

with $V_\mu = \Sigma D_\mu \Sigma^\dagger$, and D_μ being the $SU(2) \times U(1)$ -gauge-covariant derivative. The field Σ parameterizes the Goldstone sector and provides a generally nonlinear realization of the electroweak gauge symmetry [2]. In unitary gauge $\Sigma \equiv 1$ the operator V_μ reduces to

$$V_\mu = -i \frac{g_W}{\sqrt{2}} (W_\mu^+ \tau^+ + W_\mu^- \tau^-) - i g_Z Z_\mu \tau^3, \quad (3)$$

where τ^\pm and τ^3 are the generators of weak isospin group $SU(2)$. Three further operators contributing to a generic four-point-interaction are

$$\mathcal{L}_6 = \frac{\alpha_6}{16\pi^2} \text{Tr}[V_\mu V_\nu] \text{Tr}[TV^\mu] \text{Tr}[TV^\nu] \quad (4)$$

$$\mathcal{L}_7 = \frac{\alpha_7}{16\pi^2} \text{Tr}[V_\mu V^\mu] \text{Tr}[TV_\nu] \text{Tr}[TV^\nu] \quad (5)$$

$$\mathcal{L}_{10} = \frac{\alpha_{10}}{32\pi^2} [\text{Tr}(TV_\mu) \text{Tr}(TV^\mu)]^2, \quad (6)$$

which, in contrast to Eqs. (1, 2), violate $SU(2)$ via the appearance of the operator $T = \Sigma \tau^3 \Sigma^\dagger$.

These interaction terms are evaluated in three-boson-production via the processes

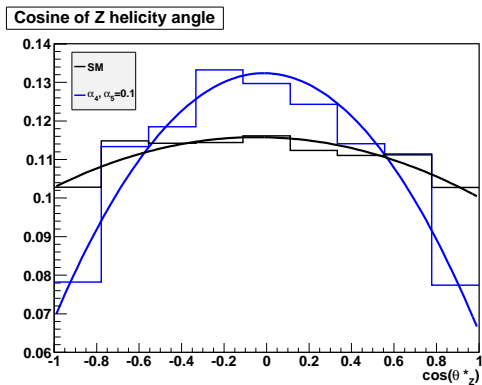
$$\begin{aligned} e^+ e^- &\longrightarrow (W^+ W^- Z) &\longrightarrow q \bar{q} q \bar{q} q \bar{q} \\ e^+ e^- &\longrightarrow (ZZZ) &\longrightarrow q \bar{q} q \bar{q} q \bar{q}. \end{aligned} \quad (7)$$

Only the sum of $SU(2)$ -conserving and -violating operators contributes to each of these processes. Hence, there will be no direct sensitivity to $SU(2)$ -violation. This question can be accessed by complementary analysis, such as W-scattering, see e. g. [4, 5]. The coupling parameters can be mapped to masses of resonant particles that may be indirectly accessible in the range of future colliders [5, 6].

The results presented here are based on previous analyses [5]. In this paper we now extend this work in two directions: First, we consider the influence of the polarization states of the bosons. This is particularly interesting since the longitudinal polarized components directly correspond to the would-be Goldstone bosons associated with the symmetry breaking pattern. Second, the restriction of considering on-shell bosons in the final state is abandoned in favor of investigating the complete set of six quark final states, corresponding to the pure hadronic decay of the intermediate bosons, which brings the overall analysis closer to the future experimental situation.

For a motivation of how the helicity angle may improve sensitivity we show Fig. 1, presenting the reconstructed

FIG. 1: Reconstructed differential cross sections normalized to the SM cross section.



helicity distribution in dependence of the anomalous coupling parameters. We have chosen $\alpha_4 = \alpha_5 = 0.1$ and compare the helicity distributions implied by taking into account the anomalous couplings to the one of the standard model. The distribution for $\cos\theta_Z^*$ are given after reconstruction as explained in the next sections.

To guide the eye the histogram has been fitted by a simple second order polynomial. From inspection of Fig. 1 it is obvious that the appearance of anomalous couplings change the shape of the distribution from a rather flat one to a more pronounced distribution. Although the helicity state of the intermediate boson is not reconstructed this way it is possible to take into account the effects of the intermediate state of polarization.

The helicity angle is given with respect to the rest system of the decaying boson, in this case the Z boson in WWZ intermediate states. To this end the co-ordinate system is properly boosted utilizing the reconstructed momenta (subject to kinematical fit).

The curves in Fig. 1 are normalized to the respective total number of events to separate effects on total cross section from variations in the distribution itself.

II. ANALYSIS LAYOUT

We analyze intermediate three-boson-production at a center-of-mass energy of $\sqrt{s} = 1$ TeV. The total integrated luminosity is assumed to be $\int \mathcal{L} = 1000 \text{ fb}^{-1}$. An earlier analysis has shown [4] that the sensitivity increases remarkably by using polarized initial e^+e^- -states. We therefore focus on the situation with 80 % right handed polarization of electrons and 60 % left handed polarization of positrons that has been the most favorable scenario. The degree of polarization has been carried over from our earlier analysis.

We consider all the six quark final states listed in Tab. I.

Each of the flavor final states is equivalent by a large number of Feynman graphs. They contain the signal events as well as a huge amount of background arising

TABLE I: Generated six quark production processes at $\sqrt{s} = 1$ TeV considered in the analysis. (Cross sections including numerical errors are given).

out state	intermediate state	σ_{tot} [fb]
$d\bar{d}d\bar{d}d$	ZZZ	$(1.886 \pm 0.011) \cdot 10^{-2}$
$d\bar{d}d\bar{u}d$	WWZ	0.228 ± 0.005
$d\bar{d}d\bar{s}s$	ZZZ	$(5.51 \pm 0.05) \cdot 10^{-2}$
$d\bar{d}d\bar{c}c$	ZZZ	$(8.80 \pm 0.07) \cdot 10^{-2}$
$d\bar{d}d\bar{b}b$	ZZZ	$(7.24 \pm 0.04) \cdot 10^{-2}$
$d\bar{d}d\bar{u}sc$	WWZ	$0,1442 \pm 0.0006$
$d\bar{d}s\bar{c}du$	WWZ	0.1449 ± 0.0009
$d\bar{u}d\bar{u}u$	WWZ	0.221 ± 0.005
$d\bar{u}d\bar{u}s$	WWZ	0.277 ± 0.005
$d\bar{u}d\bar{u}c$	WWZ	0.339 ± 0.007
$d\bar{u}d\bar{u}b$	WWZ, tt	17.72 ± 0.04
$d\bar{d}s\bar{s}s$	ZZZ	$(5.95 \pm 0.11) \cdot 10^{-2}$
$d\bar{d}s\bar{c}sc$	WWZ	0.300 ± 0.008
$d\bar{d}s\bar{s}bb$	ZZZ	0.1471 ± 0.0016
$d\bar{d}c\bar{c}c$	ZZZ	0.1157 ± 0.0023
$d\bar{d}c\bar{c}bb$	ZZZ	0.2231 ± 0.0027
$d\bar{d}b\bar{b}b$	ZZZ	$(8.10 \pm 0.06) \cdot 10^{-2}$
$d\bar{u}u\bar{u}sc$	WWZ	0.1317 ± 0.0005
$d\bar{u}s\bar{s}c$	WWZ	0.1440 ± 0.0009
$d\bar{u}s\bar{c}bb$	WWZ, tt	17.548 ± 0.029
$d\bar{u}s\bar{c}cc$	WWZ	0.1316 ± 0.0006
$u\bar{u}d\bar{u}sc$	WWZ	0.1317 ± 0.0005
$s\bar{s}d\bar{u}sc$	WWZ	0.1448 ± 0.0005
$s\bar{c}d\bar{u}c$	WWZ	0.1324 ± 0.0007
$s\bar{c}d\bar{u}b$	WWZ, tt	17.60 ± 0.04
$u\bar{u}u\bar{u}u$	ZZZ	$(4.53 \pm 0.03) \cdot 10^{-2}$
$u\bar{u}u\bar{u}s$	ZZZ	0.1152 ± 0.0012
$u\bar{u}u\bar{u}c$	ZZZ	0.1374 ± 0.0015
$u\bar{u}u\bar{u}b$	ZZZ	0.1430 ± 0.0009
$u\bar{u}s\bar{s}s$	ZZZ	$(8.54 \pm 0.12) \cdot 10^{-2}$
$u\bar{u}s\bar{c}sc$	WWZ	0.356 ± 0.012
$u\bar{u}s\bar{s}bb$	ZZZ	0.2206 ± 0.0021
$u\bar{u}c\bar{c}c$	ZZZ	0.131 ± 0.004
$u\bar{u}c\bar{c}bb$	ZZZ	0.281 ± 0.006
$u\bar{u}b\bar{b}b$	ZZZ	0.1215 ± 0.0007
$s\bar{s}s\bar{s}s$	ZZZ	$(1.926 \pm 0.014) \cdot 10^{-2}$
$s\bar{s}s\bar{s}c$	ZZZ	0.2269 ± 0.0022
$s\bar{s}s\bar{s}b$	ZZZ	$(7.26 \pm 0.05) \cdot 10^{-2}$
$s\bar{s}c\bar{c}c$	ZZZ	0.234 ± 0.006
$s\bar{s}c\bar{c}bb$	WWZ, tt	17.77 ± 0.04
$s\bar{s}b\bar{b}b$	ZZZ	$(8.11 \pm 0.06) \cdot 10^{-2}$
$c\bar{c}c\bar{c}c$	ZZZ	$(4.55 \pm 0.04) \cdot 10^{-2}$
$c\bar{c}c\bar{c}bb$	ZZZ	0.1416 ± 0.0009
$c\bar{c}b\bar{b}b$	ZZZ	0.1215 ± 0.0009
$b\bar{b}b\bar{b}b$	ZZZ	$(2.638 \pm 0.011) \cdot 10^{-2}$

from (a few thousand) standard model graphs with the same in and out states but without any quartic gauge couplings. (Note, however, that the actual generator algorithm differs from evaluating Feynman graphs, but using technique described closer in [7])

The dominating part of this background stems from direct top production, via

$$e^+e^- \rightarrow t\bar{t} \rightarrow q\bar{q}q\bar{q}b\bar{b}, \quad (8)$$

which manifests itself as a six-jet-topology. They are indicated as tt in Tab. I.

An additional type of background is related to misidentification. In case of the ZZZ intermediate states, also the contamination of reconstructed Z s with misidentified W s has to be taken into account. Particle misidentification amounts to 8% of all reconstructed Z s. The converse case (Z identified as W in reconstructed WWZ events) is less important, since the ZZZ production is largely suppressed compared to WWZ production.

The generation of events is achieved by using WHIZARD [8] and PYTHIA [9] is utilized for fragmentation to hadronic final states. Initial state radiation (ISR) has been taken into account. In order to reduce statistical fluctuations, the number of analyzed events is increased by a factor of hundred of the expected number (assuming a luminosity of $\mathcal{L} = 1000 \text{ fb}^{-1}$ at the ILC) and finally renormalized. This procedure leads to a more reliable figure of merit for the sensitivity. Subsequent detector simulation is done with the fast simulation tool SIMDET [10].

A. Fit Method

We use a χ^2 -fit to extract information on anomalous couplings from the distribution of kinematical variables

$$\chi^2 = \sum_{ijklmn} \frac{\left(N_{ijklmn}^{\text{th}}(\alpha_4, \alpha_5) - N_{ijklmn}^{\text{exp}} \right)^2}{\sigma_{ijklmn}^2}. \quad (9)$$

The indices $ijklmn$ stand for the discretized phase space variables, which are six in number, and are used to describe the event. They will be dropped in the following formulas for convenience. Confidence levels for α_4 and α_5 are calculated with MINUIT [11]. The kinematical variables, the distributions of which are sensitive observables to anomalous quartic gauge couplings and are therefore used in the analysis, are

- the invariant mass $M_{WZ} = \sqrt{(p_{W_1} + p_Z)^2}$ of the W_1 - Z -subsystem
- the invariant mass $M_{WW} = \sqrt{(p_{W_1} + p_{W_2})^2}$ of the W_1 - W_2 -subsystem
- the cosine $\cos\theta$ of Z momentum w.r.t. the beam axis
- the helicity angle of each boson: $\theta_{W_1}^*, \theta_{W_2}^*, \theta_Z^*$.

Since the bosons are off-shell, there are no self-energy corrections due to AQGC at NLO. Such contributions only arise at NNLO via loop-graphs including at least one AQGC-vertex. So in the considered order of perturbation theory there are no changes in the energy-momentum-relations compared to the SM, hence off shell effects do not lead to additional kinematical variables.

The cross section $d\sigma^{\text{NLO}}$ in NLO is of second order in the coupling constants α_i since the processes (7) contain at most one vertex with AQGC,

$$d\sigma^{\text{NLO}} = d\sigma^{\text{SM}} + \sum_i d\sigma_i^{\text{int}}\alpha_i + \sum_{k\ell} d\sigma_{k\ell}^{\text{ac}}\alpha_k\alpha_\ell. \quad (10)$$

Here $d\sigma^{\text{SM}}$ denotes the standard model contributions, $d\sigma^{\text{int}}$ the interference term linear in α , and $d\sigma^{\text{ac}}$ the quadratic term containing only AQG-vertices. The full information on the dependence on anomalous gauge couplings is incorporated in at most 5 different event dependent parameters, viz.

$$\frac{d\sigma^{\text{NLO}}}{d\sigma^{\text{SM}}} = 1 + A\alpha_4 + B\alpha_4^2 + C\alpha_5 + D\alpha_5^2 + E\alpha_4\alpha_5, \quad (11)$$

where the parameters A, \dots, E depend on the kinematical variables, but not on anomalous couplings. They can be obtained by re-weighting the SM matrix elements at five different points in the α_4 - α_5 -plane for a fixed event sample and solving the respective system of linear equations obtained from Eq. (11). We choose $\alpha_4 = \pm 0.1, \alpha_5 = 0$; $\alpha_4 = 0, \alpha_5 = \pm 0.1$, and $\alpha_4 = \alpha_5 = 0.1$. The resulting χ^2 is an analytic function of α_i due to (11) and can easily be minimized.

B. Particle Identification and Cuts

All processes used in the analysis are listed in Tab. I. In the following, for convenience and also historic reasons, processes that contain intermediate $t\bar{t}$ -production are referred to as “background”, whereas those containing intermediate boson states only are termed “signal” events. In fact kt production vastly dominates the triple boson production by two orders of magnitude (see Tab. I). Note that a negligible fraction of three boson production is also included in the “background”, since they cannot (at generator level) be separated from each other in a six quark production.

Due to hadronization the six quark final states form jets. Jet identification is done using the Durham algorithm [10]. In addition, we require a cut on the jet energy $E_{\text{jet}} > 5 \text{ GeV}$ and an upper bound on missing energy and momentum $E_{\text{mis}}^2 + p_{\perp}^2 < (65 \text{ GeV})^2$ to accept only well defined jets. The reconstructed jet momenta are pairwise combined to form invariant masses $M_{\text{jetpairs}} = \sqrt{(p_{j1} + p_{j2})^2}$ of the boson candidates. Tops are reconstructed via b-decay combining 3 jets and requiring two of them to form a W . Cuts on respective invariant masses used to identify vector bosons and top quarks are given in Tab. II and Fig. 2 Invariant masses of accepted candidates are required to have a minimum deviation from the nominal masses $M_W = 80.403 \text{ GeV}$, $M_Z = 91.1876 \text{ GeV}$, and $M_t = 174.2 \text{ GeV}$ as given in [12].

For background identification we cut on the energy E and momentum p distribution of the top candidates in

particle	lower limit	upper limit
W	$M_W - 7.5 \text{ GeV}$	$(M_W + M_Z)/2$
Z	$(M_W + M_Z)/2$	$M_Z + 7.5 \text{ GeV}$
t	$M_t - 15 \text{ GeV}$	$M_t + 15 \text{ GeV}$

TABLE II: Mass cuts used for particle reconstruction.

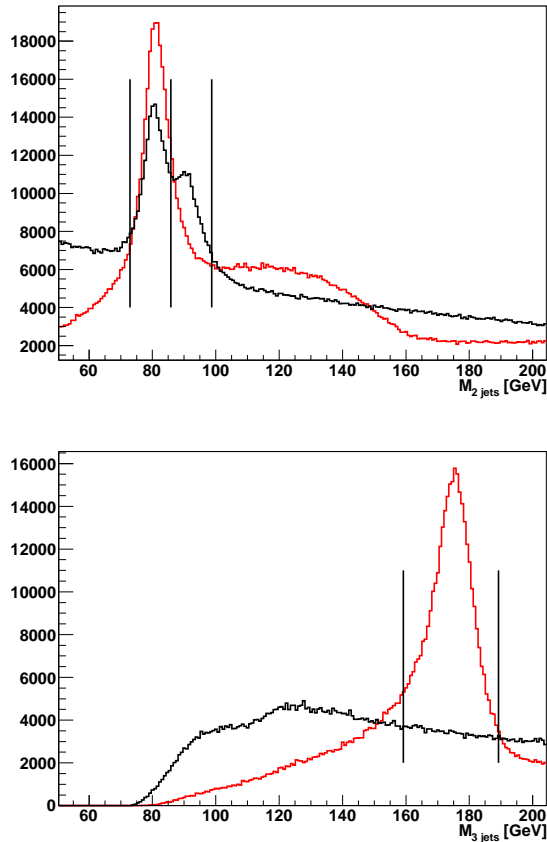
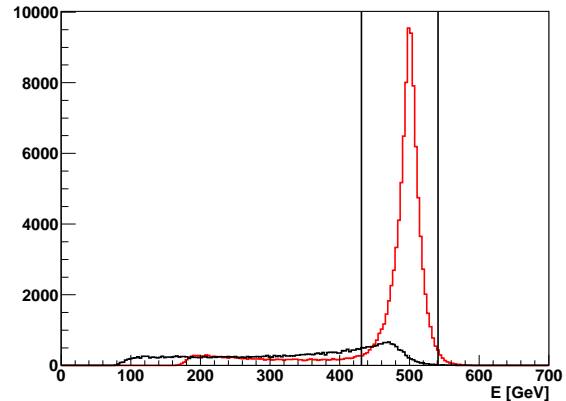


FIG. 2: The upper figure shows the invariant mass of jet pairs from which the bosons are reconstructed for background (red) and events without tt -production (black). The vertical lines indicate the selection parameters $M_W = 72.9 \text{ GeV} \dots 85.8 \text{ GeV}$, $M_Z = 85.8 \text{ GeV} \dots 98.7 \text{ GeV}$. Tops are reconstructed by combining the best W in the event with all remaining jets and selected as indicated by the vertical lines in the lower figure $|M_t - M_t^{\text{nom}}| \leq 15 \text{ GeV}$.

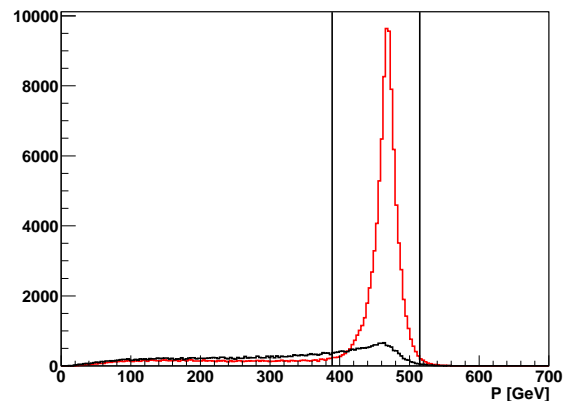
the event as shown in Fig. 3. As “signal” events, only those are included that do not contain any contributions from $t\bar{t}$ -production, whereas the “background” consists to the largest part of such events.

To enforce conservation laws a kinematical fit is applied, which minimizes the missing energy and momentum constrained by the reconstructed mass, i.e. the following expression for the reconstructed particles (reco) is minimized

$$\sum_{\text{reco}} \left\{ \frac{E_{\text{mis}}^2}{\sigma_E^2} + \sum_{i=1}^3 \frac{P_{\text{mis},i}^2}{\sigma_{P_i}^2} + \left(\frac{E_{\text{mis}}^2 - P_{\text{mis}}^2 - M_{\text{rec}}^2}{\sigma_M^2} \right)^2 \right\}$$



(a) Energy distribution of signal (black) and background (red).



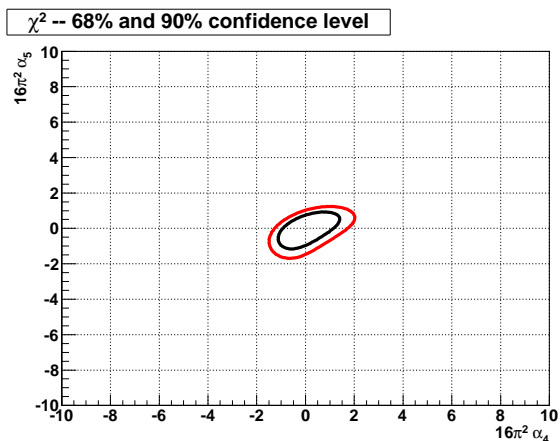
(b) Momentum distribution of signal (black) and background (red).

FIG. 3: The cuts applied to top candidates after detector simulation are shown: $|E - 486 \text{ GeV}| \leq 55 \text{ GeV}$, $|p - 452 \text{ GeV}| \leq 63 \text{ GeV}$. These numbers are mean values obtained from Monte Carlo simulation of background events $e^+e^- \rightarrow t\bar{t}$. The plots show (a) the E and (b) the p distribution from tt background (red curve) and from the WWZ signal (black curve).

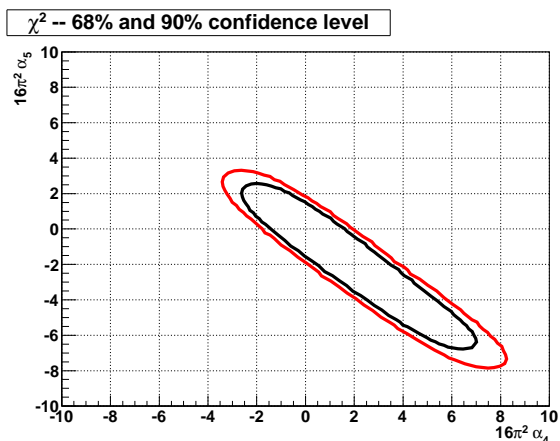
with respect to $E_{\text{mis}}, \vec{p}_{\text{mis}}$, where $E_{\text{mis}} = \sqrt{s} - E_{\text{visible}}$, $\vec{p}_{\text{mis}} = -\vec{p}_{\text{visible}}$.

III. SENSITIVITIES

As a measure of sensitivity we use the $1\text{-}\sigma$ standard deviations of the α parameters obtained from minimizing χ^2 of Eq. (9) with a SM distribution as null hypothesis. Here, we implicitly assume that the standard deviations (sensitivities) do not depend on the actual values of the anomalous couplings. This is reasonable as long as the true values for the anomalous couplings are unknown and are at least expected to lie within the range where the effective theory approach is feasible. The resulting contour



(a) WWZ



(b) ZZZ

FIG. 4: Obtained sensitivity for reconstructed events. Inner and outer contour delineate 68 % and 90 % confidence level, respectively.

gives an estimation of the maximum probability that a measured event distribution is compatible with the null hypothesis. The sensitivities obtained by this procedure are shown in Fig. 4 for intermediate WWZ and intermediate ZZZ events, respectively. The combined χ^2 fit using reconstructed WWZ and ZZZ events can be found in Fig. 5. Tab. III shows the $1\text{-}\sigma$ standard deviation for the coupling parameters calculated from Minuit.

		Ref. [5]	this work, 6 quarks		
			WWZ	(WWZ)	(ZZZ) combined
$16\pi^2\alpha_4$	σ^-	-3.53	-1.49	-1.87	-0.68
	σ^+	1.90	2.02	5.08	0.95
$16\pi^2\alpha_5$	σ^-	-1.64	-1.69	-5.20	-0.71
	σ^+	3.94	1.24	1.85	0.60

TABLE III: $1\text{-}\sigma$ standard deviations for α_4 and α_5 obtained from reconstructed WWZ, ZZZ events and from a combined fit. The lower table shows the previously obtained results (taken from [5]).

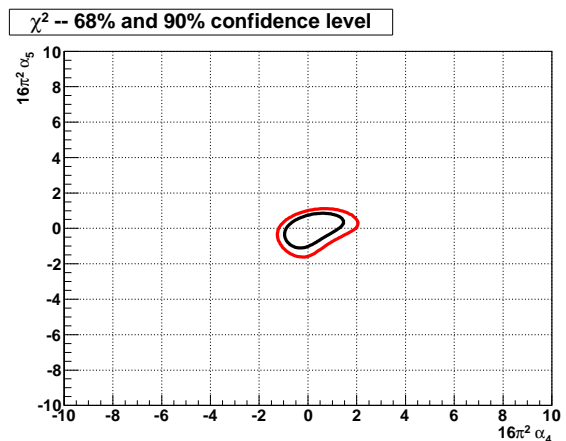


FIG. 5: Combined fit from reconstructed WWZ and ZZZ events.

IV. CONCLUSION

Based on our previous analysis the sensitivity on quartic gauge couplings of processes at the ILC involving three intermediate bosons have been improved. The improvement has been in two directions: First we have included observables related to the polarization of the intermediate bosons. This leads to a better sensitivity compared to the previous results. Second, we have utilized full six quark final states in the event generation that became available only recently. Matrix elements of all six fermion final states that can be accessed in the 1 TeV range have been included. This leads to a more realistic description of the processes closer to the expected experimental behaviour. It also leads to a more realistic treatment of background events compared to former analysis where only non-interfering tt -production has been assumed.

Of all possible generic quartic gauge couplings the production of intermediate three boson states WWZ and ZZZ is sensitive to the ones involving α_4/α_6 , and α_5/α_7 . The present analysis is done for the ILC with the option for initial state polarization. Due to the large number of events that have to be considered, we have merely favored a scenario of fully polarized initial states that has been the most sensitive case in our previous analysis [5]

Presently, we have only utilized hadronic decays. These amount to 32% of the total events with intermediate three bosons. A more complete investigation including semileptonic decays, i.e. $e^+e^- \rightarrow (VVZ) \rightarrow 4q + \ell\bar{\ell}$ is left for future work.

A next task is to combine the present analysis with the results from WW -scattering along the lines of [5] and update the characteristics of new resonant states that can be inferred from the present work.

-
- [1] Leonard Susskind. Dynamics of Spontaneous Symmetry Breaking in the Weinberg- Salam Theory. *Phys. Rev.*, D20:2619–2625, 1979.
 - [2] W. Kilian. Electroweak symmetry breaking: The bottom-up approach. *Springer Tracts Mod. Phys.*, 198:1–113, 2003.
 - [3] Anthony C. Longhitano. Low-Energy Impact of a Heavy Higgs Boson Sector. *Nucl. Phys.*, B188:118, 1981.
 - [4] P. Krstonsic, K. Monig, M. Beyer, E. Schmidt, and H. Schroder. Experimental studies of strong electroweak symmetry breaking in gauge boson scattering and three gauge boson production. 2005.
 - [5] M. Beyer et al. Determination of new electroweak parameters at the ILC: Sensitivity to new physics. *Eur. Phys. J.*, C48:353–388, 2006.
 - [6] W. Kilian and J. Reuter. Resonances and electroweak observables at the ILC. 2005.
 - [7] Mauro Moretti, Thorsten Ohl, and Jurgen Reuter. O’Mega: An optimizing matrix element generator. 2001.
 - [8] W. Kilian. WHIZARD 1.0: A generic Monte-Carlo integration and event generation package for multi-particle processes. Manual. LC-TOOL-2001-039.
 - [9] Torbjorn Sjostrand, Leif Lonnblad, Stephen Mrenna, and Peter Skands. PYTHIA 6.3: Physics and manual. 2003.
 - [10] M. Pohl and H. J. Schreiber. SIMDET - Version 4: A parametric Monte Carlo for a TESLA detector. 2002.
 - [11] F. James and M. Roos. Minuit: A System for Function Minimization and Analysis of the Parameter Errors and Correlations. *Comput. Phys. Commun.*, 10:343–367, 1975.
 - [12] W. M. Yao et al. Review of particle physics. *J. Phys.*, G33:1–1232, 2006.